Thalamo-cortical network activity during spontaneous migraine attacks

Gianluca Coppola, MD, PhD

Antonio Di Renzo

Emanuele Tinelli, MD, PhD

Cherubino Di Lorenzo, MD, PhD

Giorgio Di Lorenzo, MD, PhD

Vincenzo Parisi, MD

Mariano Serrao, MD, PhD

Jean Schoenen, MD, PhD

Francesco Pierelli, MD, PhD

Correspondence to
Dr. Coppola:
gianluca.coppola@gmail.com

ABSTRACT

Objective: We used MRI to search for changes in thalamo-cortical networks and thalamic microstructure during spontaneous migraine attacks by studying at the same time structure with diffusion tensor imaging and resting state function in interconnected brain networks with independent component analysis.

Methods: Thirteen patients with untreated migraine without aura (MI) underwent 3T MRI scans during an attack and were compared to a group of 19 healthy controls (HC). We collected resting state data in 2 selected networks identified using group independent component (IC) analysis. Fractional anisotropy (FA) values of bilateral thalami were calculated in the same participants and correlated with resting state IC Z scores.

Results: Functional connectivity between the executive and the dorso-ventral attention networks was reduced in MI compared to HC. In HC, but not in MI, the higher the IC24 Z score, encompassing interconnected areas of the dorso-ventral attention system, the lower the bilateral thalamic FA values. In patients, the higher the executive control network Z scores, the lower the number of monthly migraine days.

Conclusions: These results provide evidence for abnormal connectivity between the thalamus and attentional cerebral networks at rest during migraine attacks. This abnormality could subtend the known ictal impairment of cognitive performance and suggests that the latter might worsen with increasing attack frequency. *Neurology®* 2016;87:1–7

GLOSSARY

BOLD = blood oxygenation level–dependent; **DTI** = diffusion tensor imaging; **FA** = fractional anisotropy; **FC** = functional connectivity; **HC** = healthy controls; **IC** = independent component; **ICA** = independent component analysis; **ICHD** = International Classification of Headache Disorders; **MD** = mean diffusivity; **MI** = migraine without aura; **MPRAGE** = magnetization-prepared rapid gradient echo; **PACAP38** = pituitary adenylate cyclase-activating polypeptide-38; **ROI** = region of interest; **RS-fMRI** = resting-state functional MRI; **TE** = echo time; **TPJ** = temporoparietal junction; **TR** = repetition time; **VIP** = vasoactive intestinal polypeptide.

In recent years, various electrophysiologic data have shown that the functional brain state of migraine patients cycles up to the tipping point of an attack.[1] Ictal changes were also found in some neuroimaging studies at rest, i.e., without sensory stimulation, in particular changes in anisotropy of thalamic microstructure[2] and in gray matter density of temporo-parietal areas.[3] Besides pain and allodynia,[4] clinical symptoms during a migraine attack include cognitive disturbances,[5,6] and might be favored by malfunctioning thalamo-cortical circuits. Resting-state functional MRI (RS-fMRI) allows studying interactions between brain areas by analyzing coherence between spontaneous fluctuations of the blood oxygenation level–dependent (BOLD) signal at rest.[7] A common method to identify spatial patterns of coherent spontaneous BOLD activity—so-called functional connectivity (FC)—is independent component analysis (ICA).[8] RS-fMRI ICA explores group differences in the temporal relationship between independent, spatially distributed components.[7,9,10] The earliest RS-fMRI studies on migraine

patients were performed during attack-free periods using either an a priori selected seed-based analysis[11–15] or a single ICA approach without a priori hypothesis.[16,17] Here, we performed an RS-fMRI study using ICA to determine the FC between networks during spontaneous migraine attacks. Moreover, we combined the RS-fMRI study of the whole brain with diffusion tensor imaging (DTI) to analyze the connectivity patterns between the thalamus and various functional cerebral networks in patients at rest during an attack.

METHODS **Participants.** Out of 52 consecutive right-handed migraine without aura patients (ICHD-3 beta code 1.1) consulting our headache clinic who agreed to undergo an MRI study, 13 were scanned fortuitously during the initial 6 hours of a spontaneous full-blown migraine without aura (MI). They underwent a comprehensive battery of neuroimaging tests including RS-fMRI. We have published elsewhere the results of the DTI and voxel-based morphometry studies performed on the initial 10 patients and used these data combined with those of 3 additional patients to search for correlations with RS-fMRI.[2,3] Inclusion criteria were as follows: no history of other neurologic diseases, systemic hypertension, diabetes, or other metabolic disorders, connective or autoimmune diseases, and any other type of primary or secondary headache. Patients with fixed unilateral headaches were excluded. No preventive antimigraine drugs were allowed during the preceding 3 months. No acute antimigraine drugs were allowed until the end of the imaging session. We collected clinical data from 2-month headache diaries during the screening visit or the recording session (table). The control group comprised 19 right-handed healthy controls (HC) of comparable age and sex distribution as the migraine group. HC had no personal or family history of migraine or epilepsy or regular medication use. Female participants were scanned at midcycle. All scanning sessions were performed in the afternoon (4:00–7:00 PM). None of the recorded participants was sleep-deprived or consumed alcohol the day preceding the scans. Caffeinated beverages were not allowed on the day of scanning. A further exclusion criterion for both HC and MI was evidence of a brain lesion on structural MI.

| Table	Clinical and demographic characteristics of healthy controls (HC) and migraine patients without aura scanned during the attacks (MI)	
	HC (n = 19)	MI (n = 13)
Women, n	12	10
Age, y	31.7 ± 4.0	34.4 ± 10.7
Duration of migraine history, y		15.0 ± 9.6
Attack frequency/mo, n		3.9 ± 3.1
Attack duration, h		43.4 ± 28.4
Visual analogue scale, n		7.4 ± 0.7

Data are expressed as means ± SD.

Standard protocol approvals, registrations, and patient consents. All participants received a complete description of the study and granted written informed consent. The ethical review board of the Faculty of Medicine, University of Rome, Italy, approved the project.

Imaging protocols. All images were acquired using a Siemens (Munich, Germany) 3T Verio MRI scanner with a 12-channel head coil. Structural anatomic scans were performed using a T1-weighted sagittal magnetization-prepared rapid gradient echo (MPRAGE) series (repetition time [TR] 1,900 ms, echo time [TE] 2.93 ms, 176 sagittal slices, 0.508 × 0.508 × 1 mm³ voxels). Functional MRI data were obtained using T2*-weighted echoplanar imaging (TR 3,000 ms, TE 30 ms, 40 axial slices, 3.906 × 3.906 × 3 mm, 150 volumes). Functional BOLD data were collected with a 7 minutes 30 seconds scan during which participants were instructed to relax, avoid motion, and keep their eyes closed.

Data processing and analyses. Image data processing was performed on a personal computer using the statistical parametric mapping SPM8 software package (Wellcome Trust Centre for Neuroimaging, London, UK; fil.ion.ucl.ac.uk/spm), GIFT v3. 0, and FNC toolbox (mialab.mrn.org) in MatLab (mathwork. com). Overall the processing of imaging data was based on methods described elsewhere.[7] All images from a single participant were realigned using a 6-parameter rigid body process that was replaced with a cubic spline interpolation. The structural (T1–MPRAGE) and functional data were coregistered for each participant dataset and normalized into the standard Montreal Neurologic Institute space. This was then transformed into a common stereotactic space based on Talairach and Tournoux. Finally, functional images were spatially smoothed with an 8-mm full width half-maximum Gaussian kernel in each direction.

Component identification and selection. Grouped spatial ICA was performed for all 32 participants (HC + MI) using the Infomax algorithm. Two separate spatial ICAs were also carried out in HC and MI groups to ensure that the fluctuations of components at rest in each group were similar to those found in the total group of 32 participants (figure 1). GIFT software automatically decomposed data into 39 components. A modified version of the minimum description length criterion was adopted to determine the number of components from the aggregate dataset. Single participant spatial or temporally independent maps were then back-reconstructed from the aggregate mixing matrix.[18] We inspected all components using a priori probabilistic maps provided by GIFT and selected those corresponding to gray matter. Components located in CSF or white matter or those with low correlation to gray matter that are likely artefacts due to eye movements, head motion, and ballistic interferences were discarded. Artefacts were removed using the FNC toolbox in MatLab by applying a p value threshold of 0.01 (false discovery rate corrected). Only 2 components survived for further analysis: the executive control network (IC15) and the dorsal and ventral attention system (IC24). Before performing correlation analyses, a band-pass Butterworth filter between 0.033 and 0.13 Hz was applied on the time courses of these 2 components. Each independent component (IC) consists of a temporal waveform and an associated spatial map; the latter is expressed in terms of Z scores that reflect the degree to which a given voxel time-course correlates with the specific IC temporal waveform, which is a way to quantify the strength of the IC. To search further for a correlation between regional RS-fMRI network changes and

Figure 1 Overview of the main resting-state functional MRI findings
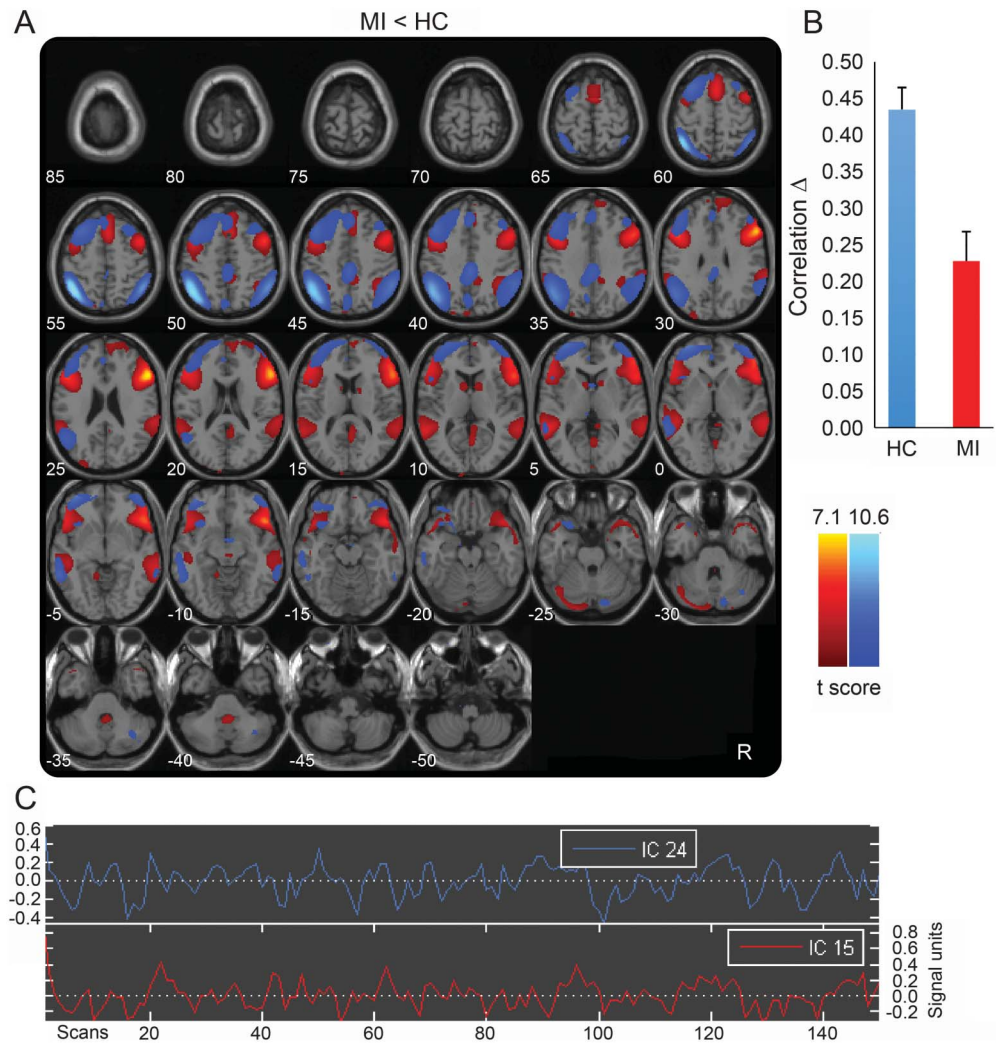
(A) Representation of the 2 independent component (IC) functional connectivity networks identified by IC analysis and differing between migraine without aura patients scanned during an attack (MI) and healthy controls (HC). All images have been coregistered into the Montreal Neurological Institute space. Brain areas are respectively colored in hot metal (IC15) or azure blue (IC24). The numbers beneath each image refer to the Z coordinate in Talairach space. (B) Reflects false discovery rate–corrected correlation between the 2 ICs, $p < 0.01$. (C) Time course of spontaneous blood oxygen level–dependent activity recorded during resting state and extracted from each of the 2 ICs.

clinical features, the mean Z max scores of each IC network were extracted and averaged for each participant.

Diffusion-weighted imaging of the thalami. DTI was acquired using single shot echoplanar imaging with a 12-channel head coil (TR 12,200 ms, TE 94 ms, 72 axial slices, 2 mm thickness, isotropic voxels). For each participant, images were obtained during the same session with diffusion gradients applied along 30 noncollinear directions with effective b values of 0 and 1,000 s/mm². Image data processing was performed with the FSL 4.0 software package (FMRIB Image Analysis Group, Oxford, UK). Diffusion data were corrected for motion and distortions caused by eddy current artefacts; the FMRIB's Diffusion Toolbox was used for local fitting of diffusion tensors, and a fractional anisotropy (FA) map was created. Two regions of interest (ROI) were defined for each participant and covered right and left thalami on each slice. The medial boundaries were determined on each slice using CSF as a landmark; the lateral

limits were verified using FA maps to exclude the internal capsule. Mean FA for every participant was obtained by averaging the values of those voxels contained in each ROI. We have previously published in extenso the results of the DTI analyses performed on the first 25 participants, 15 HC and 10 MI.[2]

Statistical analyses. Group differences for demographic data were estimated using analysis of variance. We used a 2-sample t test to detect significant differences in correlation values between the 2 independent components for HC vs MI. A conservative p value of $p < 0.01$ (correction for multiple comparisons with false discovery rate selected) was used as the significance cutoff. Connectivity combinations with statistically significant ($p < 0.01$) lag values were assessed using a 2-sample t test of the difference between averaged HC and MI patient lags. Finally, we used Pearson test to search for correlations between the MR DTI parameter FA, individual IC Z max scores, and clinical variables. p Values ≤0.05 were considered significant.

RESULTS All participants enrolled in the study completed the scanning sessions. The table summarizes the demographic and clinical characteristics of the participants. Patients reported no premonitory symptoms prior to the pain phase of migraine. None of the participants experienced pain other than headache during the scanning session. Structural brain MRIs were normal in all participants.

Resting-state fMRI. We found a difference in FC between ICs encompassing interconnected areas of the executive control network (IC15) and of the dorsal and ventral attention system (IC24) in MI patients respective to HC (figure 2). The difference was due to a lower correlation of IC pair in migraine patients during an attack. Although component directions slightly differed between HC and MI patient group, lag was not different.

DTI data. Thalamic FA values in MI patients were not different from those found in HC ($F_{1,30} = 0.200$, $p = 0.658$; $F_{1,30} = 0.031$, $p = 0.862$, respectively, for the right and for the left thalamus). Thalamic mean diffusivity (MD) values also did not differ between MI patients and HC ($F_{1,30} = 0.483$, $p = 0.492$; $F_{1,30} = 0.297$, $p = 0.589$, respectively, for the right and for the left thalamus). This is in line with our previous findings.[2]

Thalamo-cortical network correlation analysis. In HC, the higher the IC24 Z score, encompassing interconnected areas of the dorsal and ventral attention system, the lower the right and left thalamic FA values (right $r = -0.689$, $p = 0.002$; left $r = -0.526$, $p = 0.025$). Such correlations were not found in the MI group (right $r = 0.053$, $p = 0.870$; left $r = 0.039$, $p = 0.903$). In migraine patients, the higher the executive control network (IC15) Z score, the lower the monthly attack frequency ($r = -0.629$, $p = 0.029$). We found no other correlation between network Z scores and clinical features of migraine (figure 3).

DISCUSSION We found in this study that resting-state FC was decreased during an attack in migraine patients in brain networks involved in higher-order cognitive functions and attention, as compared to HCs. FC in these networks was not related to thalamic FA in patients, contrary to HCs. There was, however, a relationship between strength of connectivity in the executive network and migraine attack frequency, i.e., the lower the Z score values, the higher the attack frequency.

Recently, cerebral resting-state FC was studied in migraineurs after administration of pituitary adenylate cyclase-activating polypeptide-38 (PACAP38), which in most patients induces a migraine-like attack, or infusion of vasoactive intestinal polypeptide (VIP),

---

Figure 2   Correlation analysis 1
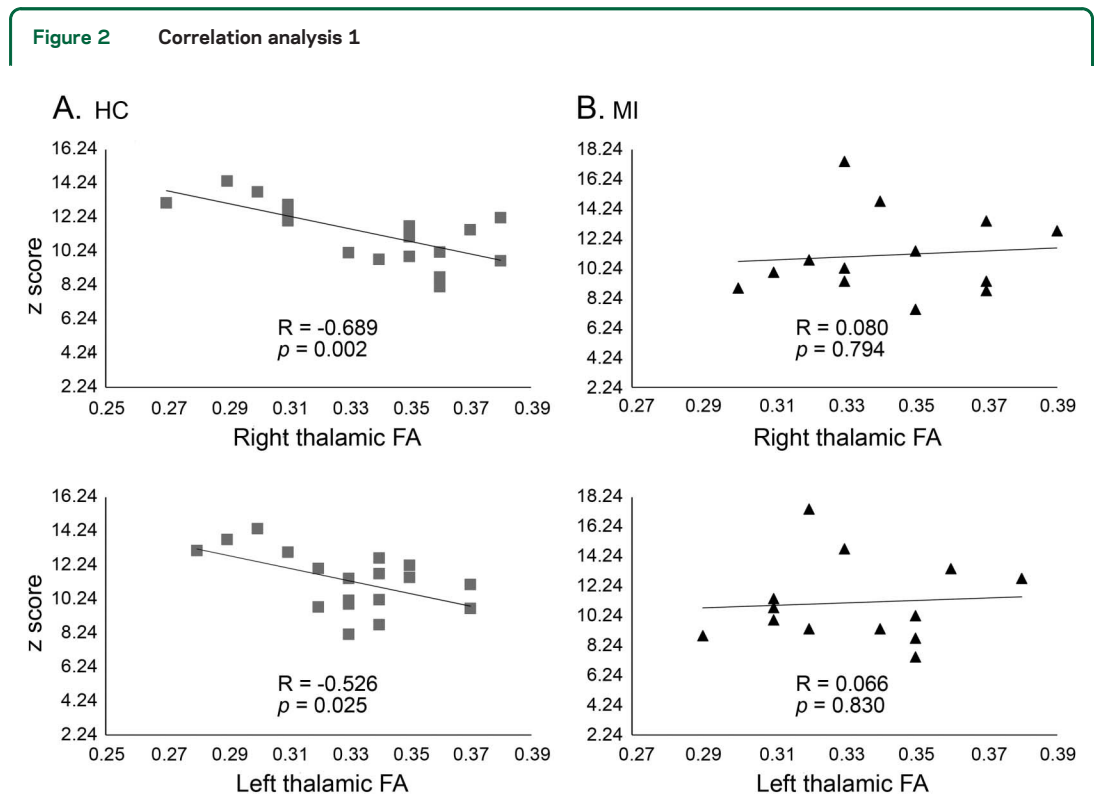
Correlations between Z score of independent component 24 (IC24) and fractional anisotropy (FA) values in right and left thalamus in HC (A) and migraine without aura patients during an attack (MI) (B). In HC, but not in MI, the higher the Z score of IC24, corresponding to the dorso-ventral attention network, the lower the bilateral thalamic FA.

Figure 3 Correlation analysis 2
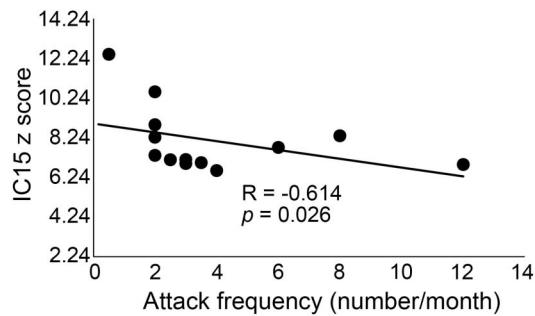
In the migraine group, we found that the higher the *Z* score of the independent component (IC)15, encompassing the executive control network, the lower the monthly attack frequency.

which has no attack-triggering effect.[19] In the early headache phase, PACAP, but not VIP, changed connectivity patterns in 3 a priori selected networks: the salience, sensorimotor, and default mode networks. This study is not directly comparable with ours for several reasons. First, we studied spontaneous, not induced, migraine attacks. Second, our recordings were made in the midst of a full-blown migraine attack, and not in the very early phase preceding the migraine-like headache. Third, we used a whole-brain ICA approach to analyze FC instead of an a priori seed-based approach.

In our study, recordings during a migraine attack were characterized by a reduction in FC between the executive control network and the dorsal and ventral attention systems. Areas of activation within the executive control network include superior and middle prefrontal cortices, anterior cingulate and paracingulate gyri, and ventrolateral prefrontal cortex.[9] The executive control network is a large-scale network that regulates higher-order cognitive functions such as working memory, goal-directed planning, complex decision-making, and endogenous attention.[20] The dorsal attention system includes the lateral occipital complex, parts of the intraparietal cortex, and middle and superior frontal gyri. It is involved in the cognitive selection of relevant sensory information, stimulus processing, and preparation of responses or action selection.[9,21,22] By contrast, activation within the ventral attention system is largely lateralized to the right hemisphere and includes the temporoparietal junction (TPJ) and inferior frontal cortex; it is recruited for the detection of behaviorally relevant sensory stimuli, particularly when they are salient and unattended.[21,22] The dorsal and ventral networks operate not only for visual information, but can also control the voluntary allocation of spatial attention towards tactile or auditory targets and hence mediate multisensory attention control.[22–25] Activity in the ventral

areas such as the TPJ was found suppressed under high sensorial load, which was interpreted as a filtering mechanism during focused attention to protect goal-driven behavior (e.g., pain or pain coping) and short-term visual memory from irrelevant distractors.[26,27] This is notably what happens in humans when the exposure to an acute stressor requires vigilant attention and impairs working memory and high-order decision-making.[20] The acute stress response is relevant for our study because headache is regarded as a strong stressor, especially when added to the high sensorial load due to migraine-associated hypersensitivity to light and sound.

Given the known functions of networks with abnormal connectivity in our study, it is not surprising that the migraine attack is associated with difficulties in multisensory attention focusing, memory retrieval, and rational decision-making. Such ictal cognitive dysfunctions have been confirmed in previous psychobehavioral studies reporting decreased performance in several cognitive domains compared to the headache-free interval: reaction time, sustained attention/concentration, working memory, visuospatial processing, language skills,[5,6] reading and processing speed, verbal memory, and learning.[28] The ictal impairment of cognitive performances may disappear with the spontaneous termination of the attack or after effective acute treatment.[6,29]

Resting-state fMRI abnormalities are at least in part dependent on migraine severity. We found that connectivity in the executive control network decreases with high attack frequency, and thus disability, and that the overall network performance may decrease with proximity to an attack.

As discussed in our previous article,[2] in gray matter areas like the thalamic nuclei, the number of neuronal connections via branching and crossing of dendritic trees, the number of local circuits, and axonal membranes contribute the most to FA, in addition to glial cells.[30] In our patients scanned during the attack, both thalami had normal FA and MD. This contrasts with the increased FA, with normal MD, which we previously observed in migraine patients scanned between attacks[2] and interpreted as reflecting shrinkage of neuronal and glial cells or gain of directional organization in combination with preserved cell density.[31,32] Interestingly, in animal models, cell shrinking may coincide with reduced neuronal electric responses.[33,34] The interictal-ictal FA changes may thus reflect changes in neuronal connections and dendritic arborizations, and hence number of local circuits that would be decreased between attacks but increase during an attack.[30]

Contrary to HC, FC in the dorso-ventral attention network was not related to bilateral thalamic anisotropy values during migraine attacks, during which

we have shown a normalization of the interictal thalamic FA increase. We postulate that the recovery of normal thalamic activity during an attack may compromise the normal reciprocal control between the thalamus and the cortex, which would amplify the ictal sensory overload leading to compensatory reduction of activity in dorso-ventral attention networks. This in turn would impair the ability to engage in goal-directed planning and complex decision-making in response to pain. That the thalamus may play a crucial role in migraine-type photophobia is supported by experimental data in rats showing convergence on posterior thalamic neurons of nociceptive trigeminovascular afferents and afferents from intrinsic light-sensitive retinal ganglion cells.[35] An abnormal thalamo-cortical control could for instance explain why there was stronger light-induced activation of the visual cortex with $H_2^{15}O$ PET in migraineurs during the attack.[36] Concordantly, we have found in previous voxel-based magnetic resonance morphometry studies that gray matter density is markedly increased during an attack in the temporal pole that has strong connexions with the thalamus.[3] Taken together, these findings suggest that an altered thalamo-cortical interaction may be a major contributor to the abnormal multimodal sensory processing during migraine attacks. However, given the complex modulation of multimodal sensory processing, we cannot exclude that other elusive factors may contribute to the abnormal thalamo-cortical interaction, for instance dysfunctional connections between brainstem centers and cortical/subcortical areas as reported between migraine attacks by others.[37]

Like most clinical studies, ours has limitations and strengths. One shortcoming because of insufficient topographic resolution is that we cannot determine if the altered thalamo-cortical connectivity results from the selective impairment of specific thalamic nuclei. Reduced volume of the central nuclear complex, the anterior nucleus, and the dorsolateral nucleus of the thalamus was found in migraine patients scanned when attack-free,[38] although the authors did not control for the occurrence of an attack after the scan. To determine whether specific thalamic nuclei or their corresponding cortical targets are responsible for the ictal impairment of thalamo-cortical networks, resting-state fMRI studies of the connectivity between cortical areas and single thalamic nuclei are necessary. Although our cohort was larger than in any other previous MRI study of spontaneous migraine attacks,[36,39–41] the relatively low number of patients and ensuing low statistical power may not have sufficed to detect more subtle abnormalities. We were unable to scan our patients also outside of an attack as their own control, which would have strengthened our conclusions. A strength

of our method is that the analysis of the dependence between pairs of functional networks allows disclosing even weak connectivity between interconnected networks.

Future work should attempt to clarify the role of the different networks in relation to MI-associated multisensory phenomena such as photophobia and allodynia. It is also seminal to search for a possible relation between the abnormal functional cortical connectivity at rest described here and the known ictal activation of brainstem nuclei.[39,41]

AUTHOR CONTRIBUTIONS

G.C. made substantial contributions to protocol development, interpretation of data, and drafting the manuscript. V.P., M.S., J.S., and F.P. were involved in the interpretation of data as well as in drafting the manuscript. F.P. and C.D.L. contributed to participant enrollment. A.D.R. and E.T. were implied in recording, data processing, analysis, and statistics.

REFERENCES

1. Coppola G, Di Lorenzo C, Schoenen J, Pierelli F. Habituation and sensitization in primary headaches. J Headache Pain 2013;14:65.
2. Coppola G, Tinelli E, Lepre C, et al. Dynamic changes in thalamic microstructure of migraine without aura patients: a diffusion tensor magnetic resonance imaging study. Eur J Neurol 2014;21:287.e13.
3. Coppola G, Di Renzo A, Tinelli E, et al. Evidence for brain morphometric changes during the migraine cycle: a magnetic resonance-based morphometry study. Cephalalgia 2015;35:783–791.
4. Burstein R, Jakubowski M, Garcia-Nicas E, et al. Thalamic sensitization transforms localized pain into widespread allodynia. Ann Neurol 2010;68:81–91.
5. Farmer K, Cady R, Bleiberg J, Reeves D. A pilot study to measure cognitive efficiency during migraine. Headache 2000;40:657–661.
6. Farmer K, Cady R, Bleiberg J, et al. Sumatriptan nasal spray and cognitive function during migraine: results of an open-label study. Headache 2001;41:377–384.

7. Jafri M, Pearlson GD, Stevens M, Calhoun VD. A method for functional network connectivity among spatially independent resting-state components in schizophrenia. Neuroimage 2008;39:1666–1681.

8. Fox M, Raichle ME. Spontaneous fluctuations in brain activity observed with functional magnetic resonance imaging. Nat Rev Neurosci 2007;8:700–711.

9. Beckmann C, DeLuca M, Devlin JT, Smith SM. Investigations into resting-state connectivity using independent component analysis. Philos Trans R Soc Lon B Biol Sci 2005;360:1001–1013.

10. Mantini D, Perrucci MG, Del Gratta C, Romani GL, Corbetta M. Electrophysiological signatures of resting state networks in the human brain. Proc Natl Acad Sci USA 2007;104:13170–13175.

11. Mainero C, Boshyan J, Hadjikhani N. Altered functional magnetic resonance imaging resting-state connectivity in periaqueductal gray networks in migraine. Ann Neurol 2011;70:838–845.

12. Jin C, Yuan K, Zhao L, et al. Structural and functional abnormalities in migraine patients without aura. NMR Biomed 2013;26:58–64.

13. Yuan K, Qin W, Liu P, et al. Reduced fractional anisotropy of corpus callosum modulates inter-hemispheric resting state functional connectivity in migraine patients without aura. PLoS One 2012;7:e45476.

14. Xue T, Yuan K, Zhao L, et al. Intrinsic brain network abnormalities in migraines without aura revealed in resting-state fMRI. PLoS One 2012;7:e52927.

15. Yuan K, Zhao L, Cheng P, et al. Altered structure and resting-state functional connectivity of the basal ganglia in migraine patients without aura. J Pain 2013;14:836–844.

16. Russo A, Tessitore A, Giordano A, et al. Executive resting-state network connectivity in migraine without aura. Cephalalgia 2012;32:1041–1048.

17. Tessitore A, Russo A, Giordano A, et al. Disrupted default mode network connectivity in migraine without aura. J Headache Pain 2013;14:89.

18. Li YO, Adali T, Calhoun VD. Estimating the number of independent components for functional magnetic resonance imaging data. Hum Brain Mapp 2007;28: 1251–1266.

19. Amin FM, Hougaard A, Magon S, et al. Change in brain network connectivity during PACAP38-induced migraine attacks: a resting-state functional MRI study. Neurology 2016;86:180–187.

20. Hermans E, Henckens M, Joëls M, Fernández G. Dynamic adaptation of large-scale brain networks in response to acute stressors. Trends Neurosci 2014;37: 304–314.

21. Corbetta M, Shulman GL. Control of goal-directed and stimulus-driven attention in the brain. Nat Rev Neurosci 2002;3:201–215.

22. Vossel S, Geng JJ, Fink GR. Dorsal and ventral attention systems: distinct neural circuits but collaborative roles. Neuroscientist 2014;20:150–159.

23. Driver J, Spence C. Crossmodal attention. Curr Opin Neurobiol 1998;8:245–253.

24. Macaluso E, Driver J. Multisensory spatial interactions: a window onto functional integration in the human brain. Trends Neurosci 2005;28:264–271.

25. Macaluso E. Orienting of spatial attention and the interplay between the senses. Cortex 2010;46:282–297.

26. Shulman G, Astafiev SV, McAvoy MP, d'Avossa G, Corbetta M. Right TPJ deactivation during visual search: functional significance and support for a filter hypothesis. Cereb Cortex 2007;17:2625–2633.

27. Todd J, Fougnie D, Marois R. Visual short-term memory load suppresses temporo-parietal junction activity and induces inattentional blindness. Psychol Sci 2005; 16:965–972.

28. Gil-Gouveia R, Oliveira A, Martins I. Cognitive dysfunction during migraine attacks: a study on migraine without aura. Cephalalgia 2015;35:662–674.

29. Koppen H, Palm-Meinders I, Kruit M, et al. The impact of a migraine attack and its after-effects on perceptual organization, attention, and working memory. Cephalalgia 2011;31:1419–1427.

30. Beaulieu C. The basis of anisotropic water diffusion in the nervous system: a technical review. NMR Biomed 2002; 15:435–455.

31. Wieshmann UC, Clark CA, Symms MR, Franconi F, Barker GJ, Shorvon SD. Reduced anisotropy of water diffusion in structural cerebral abnormalities demonstrated with diffusion tensor imaging. Magn Reson Imaging 1999; 17:1269–1274.

32. Mandl RC, Schnack HG, Zwiers MP, van der Schaaf A, Kahn RS, Hulshoff P. Functional diffusion tensor imaging: measuring task-related fractional anisotropy changes in the human brain along white matter tracts. PLoS One 2008;3:e3631.

33. Tasaki I, Byrne PM. Rapid structural changes in nerve fibers evoked by electric current pulses. Biochem Biophys Res Commun 1992;188:559–564.

34. Tasaki I. Rapid structural changes in nerve fibers and cells associated with their excitation processes. Jpn J Physiol 1999;49:125–138.

35. Noseda R, Kainz V, Jakubowski M, et al. A neural mechanism for exacerbation of headache by light. Nat Neurosci 2010;13:239–245.

36. Denuelle M, Boulloche N, Payoux P, Fabre N, Trotter Y, Géraud G. A PET study of photophobia during spontaneous migraine attacks. Neurology 2011;76: 213–218.

37. Tso AR, Trujillo A, Guo CC, Goadsby PJ, Seeley WW. The anterior insula shows heightened interictal intrinsic connectivity in migraine without aura. Neurology 2015; 84:1043–1050.

38. Magon S, May A, Stankewitz A, et al. Morphological abnormalities of thalamic subnuclei in migraine: a multi-center MRI study at 3 Tesla. J Neurosci 2015;35:13800– 13806.

39. Weiller C, May A, Limmroth V, et al. Brain stem activation in spontaneous human migraine attacks. Nat Med 1995;1:658–660.

40. Bednarczyk EM, Remler B, Weikart C, Nelson AD, Reed RC. Global cerebral blood flow, blood volume, and oxygen metabolism in patients with migraine headache. Neurology 1998;50:1736–1740.

41. Afridi SK, Giffin NJ, Kaube H, et al. A positron emission tomographic study in spontaneous migraine. Arch Neurol 2005;62:1270–1275.